ELSEVIER

Journal of Crystal Growth 201/202 (1999) 415–418

JOURNAL OF CRYSTAL GROWTH

MBE growth of GaN and AlGaN layers on Si(1 1 1) substrates: doping effects

M.A. Sánchez-García[a,]*, E. Calleja[a], F.B. Naranjo[a], F.J. Sánchez[a], F. Calle[a], E. Muñoz[a], A.M. Sánchez[b], F.J. Pacheco[b], S.I. Molina[b]

[a]Departmento Ingeniería Electrónica, ETSI Telecomunicación, UPM, Ciudad Universitaria s/n, 28040 Madrid, Spain

[b]Departmento de Ciencia de los Materiales e Ingeniería Metalúrgica y Química Inorgánica, Universidad de Cádiz, Apdo. 40, 11510 Puerto Real (Cádiz), Spain

Abstract

High-quality GaN layers with 8 arcmin (X-ray diffraction full-width at half-maximum, XRD FWHM) and rms surface roughness of 57 Å are grown on Si(1 1 1) substrates when using optimized AlN buffer layers. Si-doping produces n-type films reaching carrier concentrations up to 1.7×10^{19} cm^{-3} with mobilities of 100 cm^2/V s. A reduction of the lattice parameter c together with a red shift in the photoluminescence (PL) emission is observed with increasing Si doping. The dislocation density observed by plan-view transmission electron microscopy (PVTEM) also decreases by close to one order of magnitude (from 5.3×10^9 to 8×10^8 cm^{-2}) when increasing the Si doping (from 1.1×10^{17} to 6.0×10^{18} cm^{-3}). AlGaN layers were grown with Al content ranging from 10% to 76% with XRD FWHM of 22 arcmin and intense low-temperature photoluminescence. N-type doping is achieved in AlGaN (40%) with Si, reaching electron concentrations of 8×10^{19} cm^{-3}. © 1999 Elsevier Science B.V. All rights reserved.

Keywords: GaN layers; Si(1 1 1) substrates; AlN buffer layer

1. Introduction

Gallium nitride (GaN) and its related materials have received a great deal of attention in the past ten years due to their capabilities in the ultraviolet spectral range and their chemical properties [1]. However, in spite of the commercial availability of high-efficiency LEDs and the achievement of room-temperature cw operating LD [2], there are still some controversial and not-completely understood aspects in this material, for instance, the effect of Si doping in GaN.

In this work, photoluminescence (PL) and transmission electron microscopy (TEM) techniques are used to analyze the effect of the Si-doping of GaN layers on the thermal residual stress and dislocation distribution. AlGaN layers of different composition are also studied by scanning electron microscopy (SEM) and TEM to assess the crystal morphology.

---

*Corresponding author. Tel.: +34-91-5495700; fax: +34-91-3367323; e-mail: sanchez@die.upm.es.

PII: S0022-0248(98)01365-7

2. Experimental details

GaN and AlGaN films were grown on Si(1 1 1) on axis substrates by plasma-assisted molecular beam epitaxy (MBE), using a radio frequency (RF) plasma source. Details of the growth were published elsewhere [3].

Low-temperature PL was performed exciting with the 334.4 nm line of an Ar^+ laser. Cross-sectional (XTEM) and plan-view (PVTEM) micrographs were obtained with a Jeol 1200 EX microscope.

3. Results

3.1. Undoped and Si-doped GaN layers

GaN films were grown at 750°C on AlN-buffered Si(1 1 1) substrates. Optimal buffer layers (at 850°C) [4] and GaN films (at 750°C) [5] were grown using III/V ratios slightly above stochiometry. Following the two-step growth procedure for GaN layers [5] best XRD FWHM results of 8 arcmin (θ–2θ scan with open detector configuration) and rms surface roughness of 57 Å (10 μm × 10 μm scan) for a 1 μm thick GaN layer were obtained. Hall data on these samples were unreliable due to the formation of a highly p-type channel at the AlN/Si(1 1 1) interface by thermal diffusion [6]. However, *C–V* measurements, using horizontal Schottky diodes,

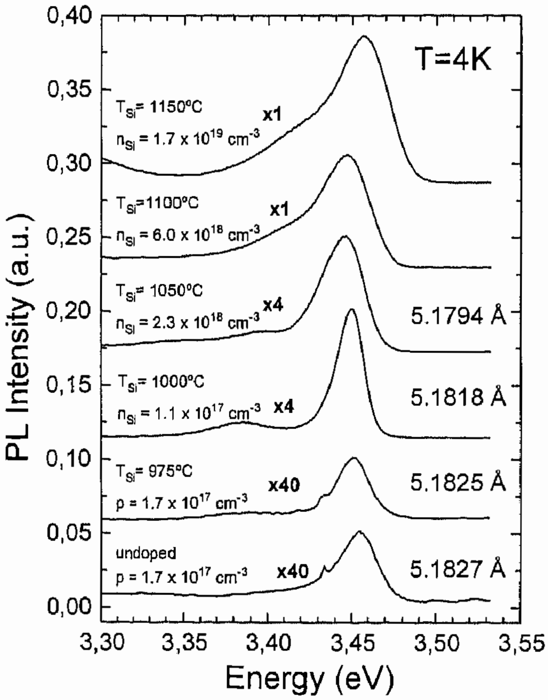

Fig. 1. Low-temperature photoluminescence of Si-doped GaN layers as a function of the Si-doping. On the right side: values of the *c*-axis lattice-constant from X-ray diffraction data.

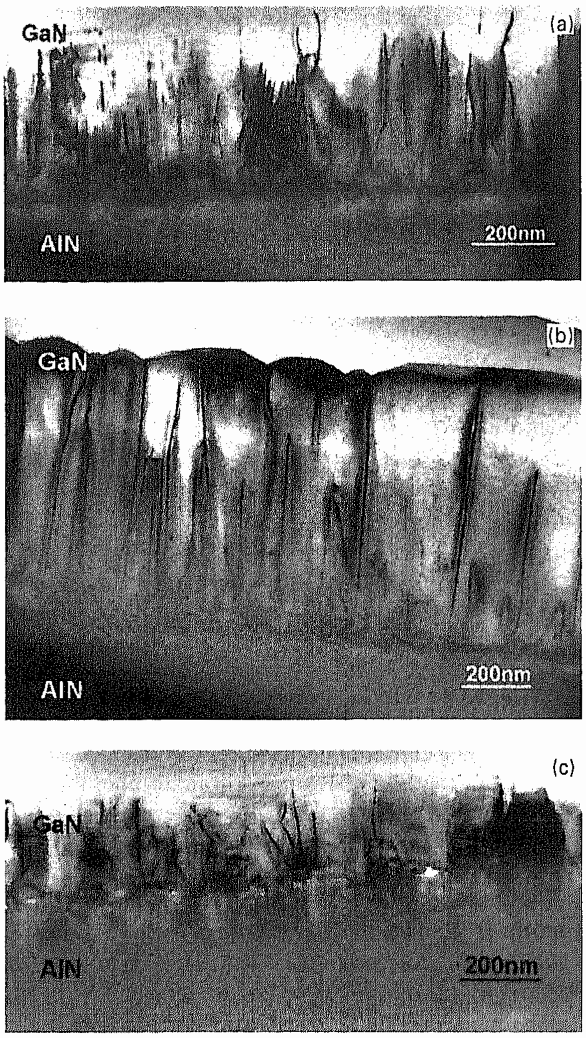

Fig. 2. XTEM photographs of GaN layers: (a) undoped GaN layer with dislocation density ρ of $6.4 \times 10^9\ cm^{-2}$, (b) Si-doped ($n = 1.1 \times 10^{17}\ cm^{-3}$) with $\rho = 5.3 \times 10^9\ cm^{-2}$, (c) $n = 6.0 \times 10^{18}\ cm^{-3}$, $\rho = 8 \times 10^8\ cm^{-2}$.

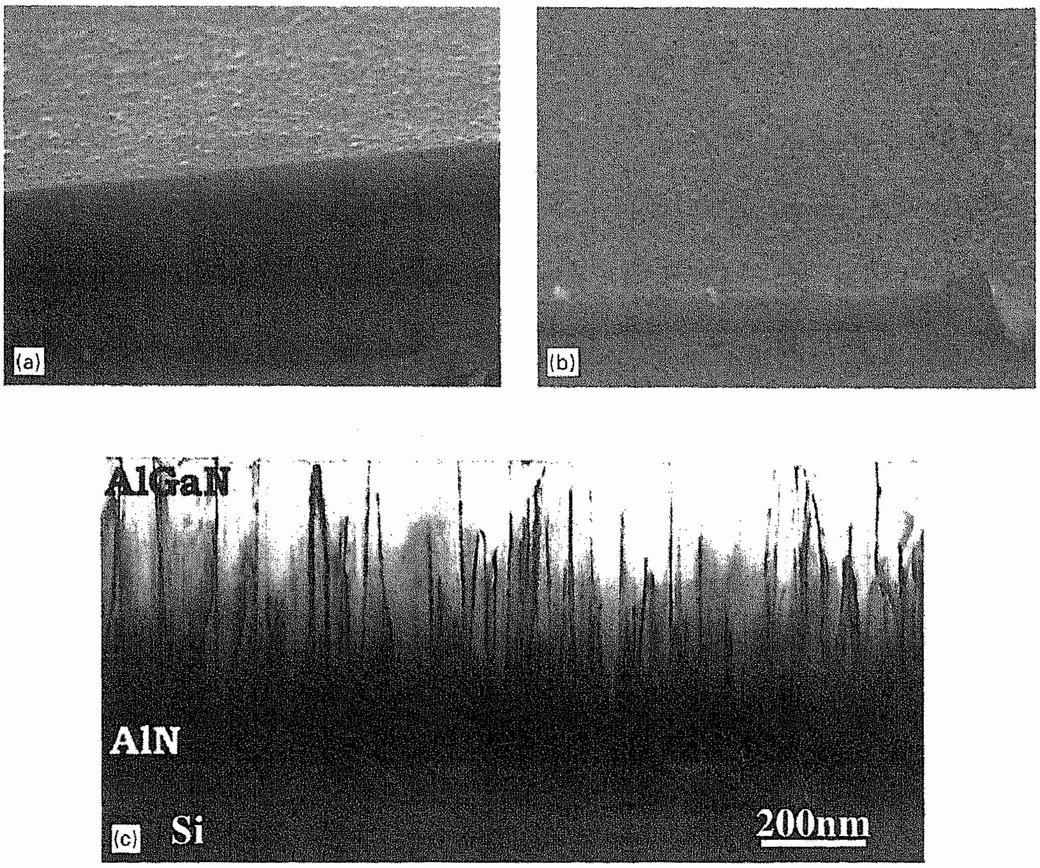

Fig. 3. SEM photographs of AlGaN layers with different Al content: (a) 11%, and (b) 76%. (c) XTEM image of an $Al_{12}Ga_{88}N$ layer showing the low free surface roughness.

lead to a residual electron concentration of 1.8×10^{17} cm^{-3}, no matter whether the Si substrate is removed by wet etching with H_3NO : HF or not.

Doping of GaN layers with Si was easily achieved, reaching electron concentrations up to 1.7×10^{19} cm^{-3}. For cell temperatures at or above 1050°C a clear n-type conductivity was measured with carrier concentrations ranging from 2×10^{18} to 1.7×10^{19} cm^{-3} and mobilities around 100 cm^2/V s. However, for cell temperatures below 1000°C and for undoped samples, an apparent p-type conductivity was measured due to the diffusion process already mentioned [6]. Fig. 1 shows low-temperature PL measurements of an undoped GaN sample and different Si-doped GaN samples. High-resolution XRD measurements on some of these samples were performed to determine the *c*-axis lattice constant as shown in Fig. 1. As the Si-doping increases, the emission around 3.45 eV shifts to lower energy and the *c* lattice-constant decreases. Both effects suggest an increase of biaxial tensile strain, indicating that Si-doping has a substantial effect on the crystal morphology, in good agreement with previous observations [7]. XTEM photographs (Fig. 2) of an undoped GaN sample and two different Si-doped samples show differences in the dislocations distribution. PVTEM images also indicate a dislocation density decrease from 6.4×10^9 cm^{-2} (undoped sample) to 8×10^8 cm^{-2} (highest doped one). This reduction can be explained due to the interaction between planar defects and dislocations which propagate along the growth direction that are bent, not allowing them to reach the free surface. A more detailed study of this mechanism and the effect of the Si-doping in the grain size and distribution is currently underway [8].

3.2. *Growth of AlGaN layers*

AlGaN layers were grown at 770°C using optimized AlN buffers, with Al content ranging from 10% to 76%. AlGaN layers exhibited XRD FWHM of 22 arcmin and very intense low-temperature PL. The growth temperature and III/V ratios are the main parameters to be optimized as a function of the Al%. A 2 × 2 surface reconstruction was observed indicating a smooth and two-dimensional growth mode. Fig. 3 (a and b) shows SEM photographs of different Al-content AlGaN layers. The Al content was determined by XRD. XTEM imaging of an $Al_{12}Ga_{88}N$ layer is shown in Fig. 3c indicating a low free surface roughness. N-type doping was easily achieved with Si, reaching electron concentrations up to 8×10^{19} cm^{-3}. Finally, AlGaN layers with Al content below 20% were employed as buffer layers for the growth of GaN, leading to even smoother surfaces (rms surface roughness of 43 Å). A better surface reconstruction (2 × 2) at the end of the AlGaN growth, as compared with the AlN buffer, and the smaller mismatch between AlGaN and GaN may explain this morphological improvement.

4. Conlusions

High quality GaN layers have been grown on Si(1 1 1) substrates with XRD FWHM of 8 arcmin and 57 Å surface roughness. Si-doping of these GaN layers produces a decrease in the *c*-axis lattice constant together with a decrease in the threading dislocation density. Both observations point to an increase in the biaxial tensile strain of the layer which is also deduced from low temperature photoluminescence. AlGaN layers have been grown with smooth surfaces, XRD FWHM of 22 arcmin and intense low-temperature PL. The use of these AlGaN layers as buffer for the growth of GaN layers leads to an improvement of the GaN crystal morphology.

Acknowledgements

This work was partially supported by CICYT Project MAT 98-0823-C03-01 and EU ESPRIT contract LTR 20968 (LAQUANI).

References

[1] S. Nakamura, G. Fasol, The Blue Laser Diode – GaN based Light Emitters and Lasers, Springer, Heidelberg, 1997.

[2] S. Nakamura, M. Senoh, S.I. Nagahama, N. Iwasa, T. Yamada, T. Matsushita, H. Kiyoku, Y. Sugimoto, T. Kozaki, H. Umemoto, M. Sano, K. Chocho. Appl. Phys. Lett. 72 (1998) 2014.

[3] M.A. Sánchez-García, E. Calleja, E. Monroy, F.J. Sánchez, F. Calle, E. Muñoz, R. Beresford, J. Crystal Growth 183 (1998) 23.

[4] E. Calleja, M.A. Sánchez-García, E. Monroy, F.J. Sánchez, E. Muñoz, A. Sanz-Hervás, C. Villar, M. Aguilar, J. Appl. Phys. 82 (1997) 4681.

[5] M.A. Sánchez-García, E. Calleja, F.J. Sánchez, F. Calle, E. Monroy, D. Basak, E. Muñoz, C. Villar, A. Sanz-Hervás, M. Aguilar, J.J. Serrano, J.M. Blanco, J. Electron. Mater. 27 (1998) 276.

[6] E. Calleja, M.A. Sánchez-García, D. Basak, F.J. Sánchez, F. Calle, P. Youinou, E. Muñoz, J.J. Serrano, J.M. Blanco, C. Villar, T. Laine, J. Oila, K. Saarinen, P. Hautojarvi, C.H. Molloy, D.J. Somerford, I. Harrison, Phys. Rev. B 58 (1998) 1550.

[7] S. Ruvimov, Z. Liliental-Weber, T. Suski, J.W. Ager III, J. Washburn, J. Krueger, C. Kisielowski, E.R. Weber, H. Amano, I. Akasaki, Appl. Phys. Lett. 69 (1996) 990.

[8] S. I. Molina, A. M. Sanchez, F. J. Pacheco, R. Garcia, M. A. Sanchez-Garcia, E. Calleja, to be published.